

## Supporting Information

# Nanometer-Scaled Surface Roughness of a 3-D Cu Substrate Promoting Li Nucleation in Li-Metal Batteries

*Taegyu Jang<sup>a</sup>, Jinhyuk Kang<sup>a</sup>, Sujung Kim<sup>a</sup>, Minyoung Shim<sup>a</sup>, Jiyong Lee<sup>b</sup>, Jongchan Song<sup>b</sup>, Wonkeun Kim<sup>b</sup>, Kyoungghan Ryu<sup>b</sup> and Hye Ryung Byon<sup>a\*</sup>*

<sup>a</sup>Department of Chemistry, Korea Advanced Institute of Science and Technology (KAIST), and Advanced Battery Center, KAIST Institute for NanoCentury, Daejeon 34141, Republic of Korea.

<sup>b</sup>Institute of Fundamental & Advanced Technology (IFAT), Research & Development Division, Hyundai Motor group, 37, Cheoldobangmulgwan-ro, Uiwang-Si, Gyeonggi-Do, 16082, Republic of Korea.

\*E-mail: [hrbyon@kaist.ac.kr](mailto:hrbyon@kaist.ac.kr)

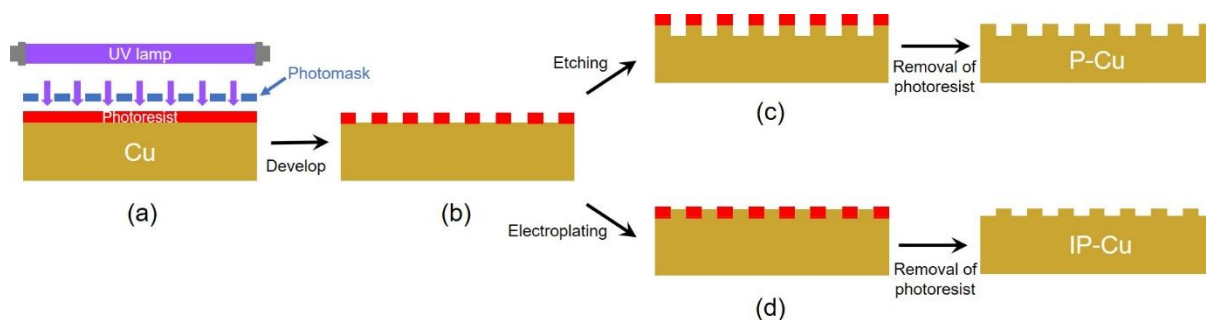


**Figure S1.** Schematic illustration of P-Cu and IP-Cu preparation. (a) UV light irradiation, (b) developing, (c) chemical etching of Cu foil and removal of photoresist to prepare P-Cu, (d) electrochemical Cu plating and removal of photoresist to fabricate IP-Cu.

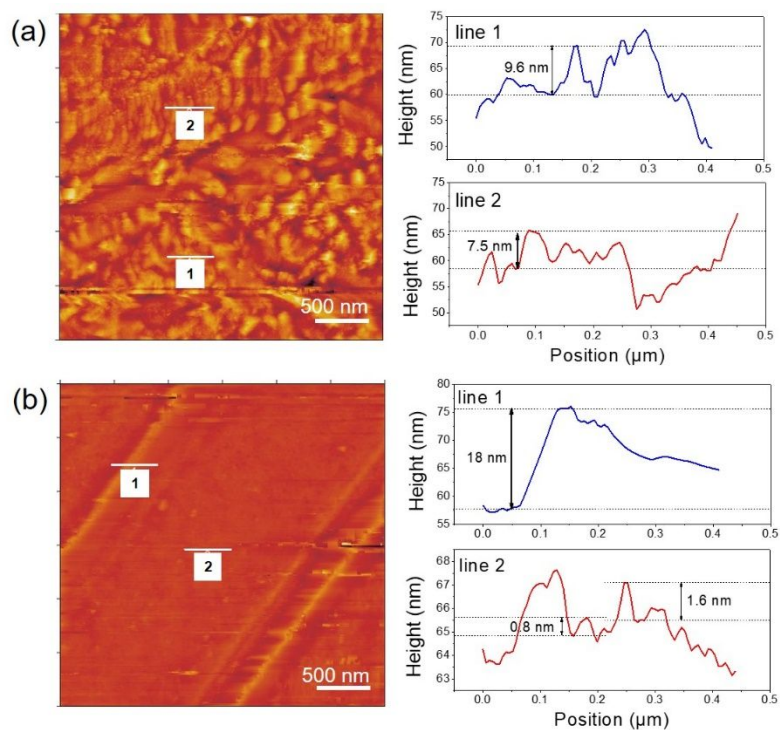


**Figure S2.** Topographic AFM images of (a) etched region and (b) squared-pattern region in P-Cu. The right panels are height profiles of line 1 and 2 in the corresponding AFM images. The long and linear patterns having  $\sim 20$  nm height at the line 1 in (b) are often observed from the as-received Cu foil.

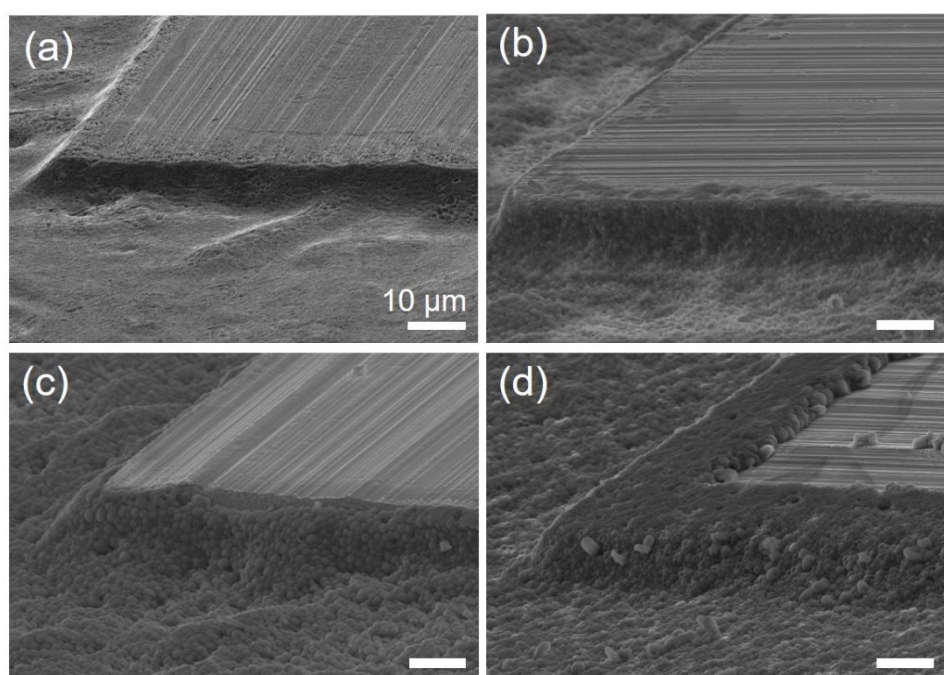


**Figure S3.** High-magnification SEM images of P-Cu at (1) as-prepared state, (b) 0.1 mAh cm<sup>-2</sup> (c) 0.3 mAh cm<sup>-2</sup> (d) 0.5 mAh cm<sup>-2</sup> capacity. Galvanostatic tests were carried out at a current density of 2 mA cm<sup>-2</sup>. All scale bars are 10 μm.

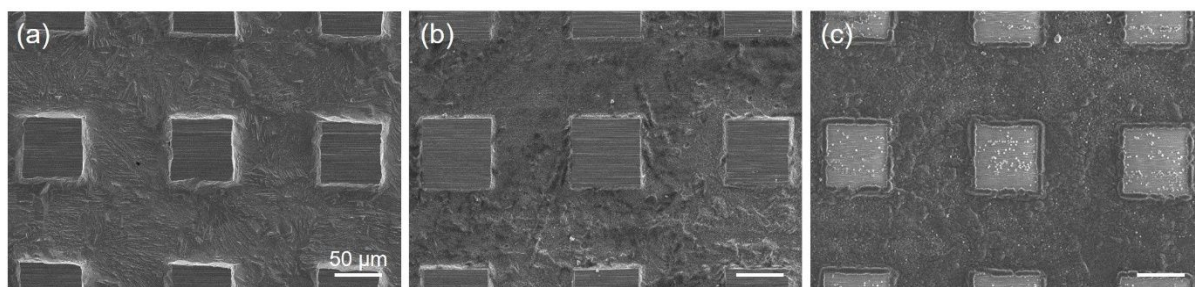


**Figure S4.** SEM images of P-Cu with  $80 \times 80 \mu\text{m}^2$  pattern at (a) as-prepared statement, (b)  $0.1 \text{ mAh cm}^{-2}$ , (c)  $0.5 \text{ mAh cm}^{-2}$ . Galvanostatic tests were carried out at a current density of  $2 \text{ mA cm}^{-2}$ . All scale bars indicate  $50 \mu\text{m}$ .



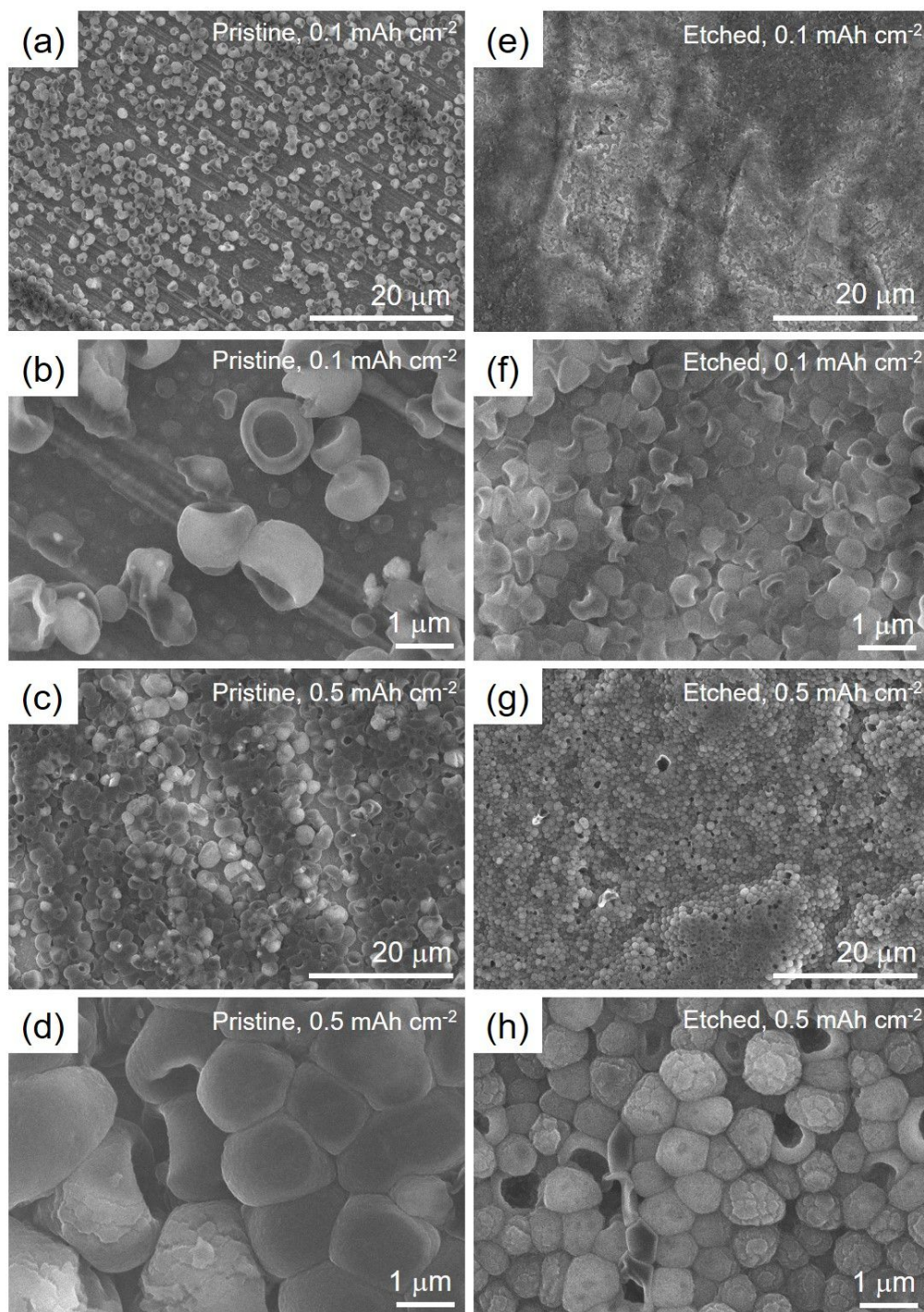


**Figure S5.** SEM images of (a-d) pristine Cu foil and (e-h) etched Cu substrates after (a, b, e, f) 0.1 mAh cm<sup>-2</sup> and (c, d, g, h) 0.5 mAh cm<sup>-2</sup> capacity. Galvanostatic tests were carried out at a current density of 2 mA cm<sup>-2</sup>.

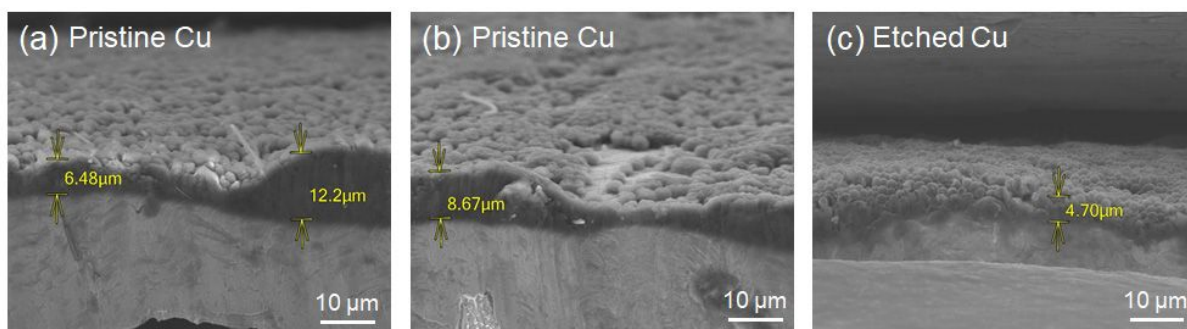


**Figure S6.** Cross-sectional SEM images of Li deposition on (a-b) pristine Cu and (c) etched Cu substrates after plating at  $0.5 \text{ mAh cm}^{-2}$  with a current density of  $2 \text{ mA cm}^{-2}$ .

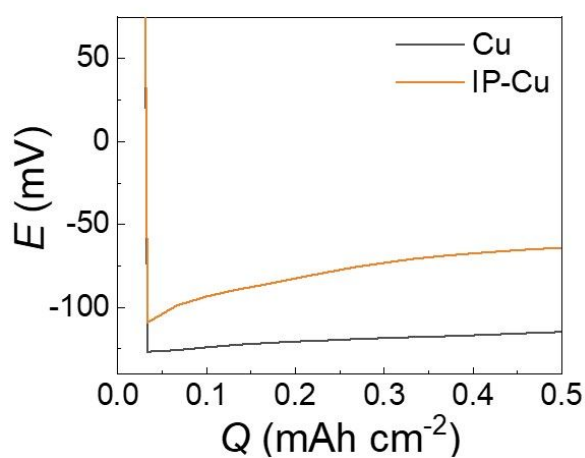


**Figure S7.** Comparative galvanostatic voltage profiles of IP-Cu (yellow) and pristine Cu foil (black) for the 1<sup>st</sup> Li plating process at a current density of  $2 \text{ mA cm}^{-2}$ .

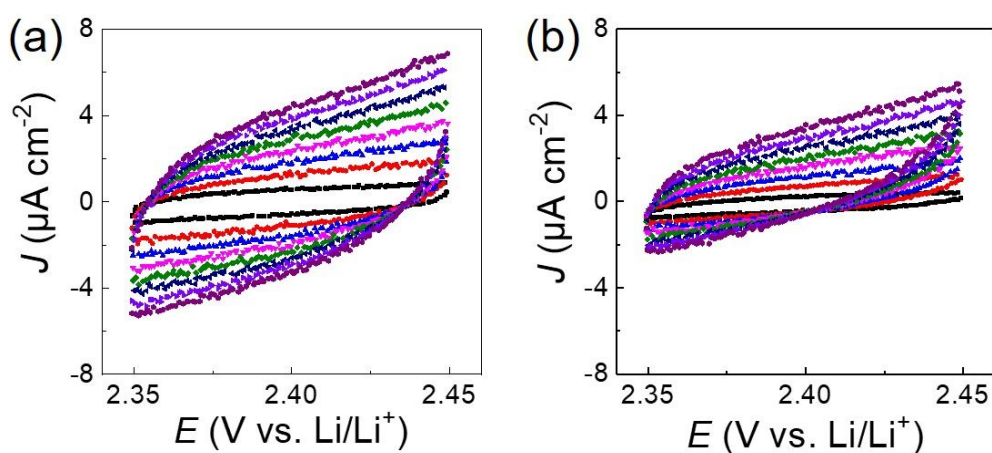


**Figure S8.** CV cycles of (a) etched Cu and (b) pristine Cu to measure EDLC. Scan rates were 4 (black), 8 (red), 12 (blue), 16 (pink), 20 (green), 24 (navy), 28 (light purple), and 32  $\text{mV s}^{-1}$  (dark purple). The potential range was 2.35~2.45 V, where Faradaic reaction does not occur.

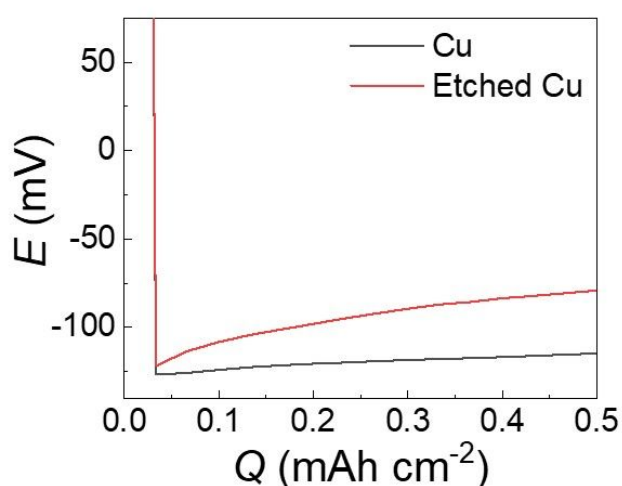


**Figure S9.** Comparative galvanostatic voltage profiles of etched Cu (red) and pristine Cu foil (black) for the 1<sup>st</sup> Li plating process at a current density of 2  $\text{mA cm}^{-2}$ .



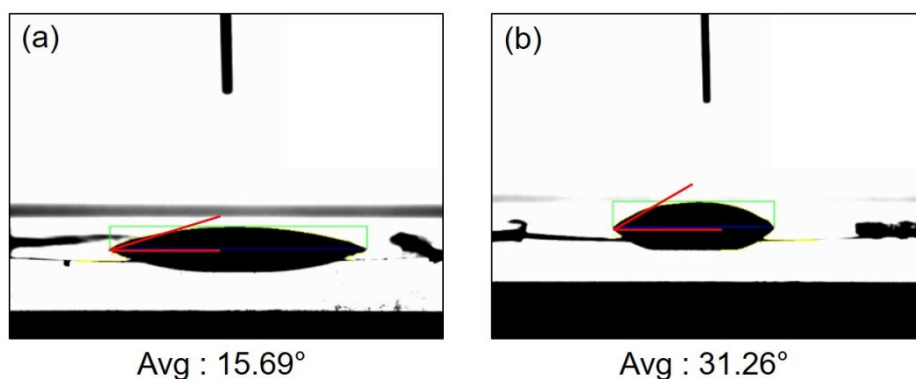


**Figure S10.** Representative contact-angle images of 1 M LiTFSI in DOL/DME with 1 wt% LiNO<sub>3</sub> electrolyte solution on (a) etched Cu and (b) pristine Cu in ambient atmosphere.

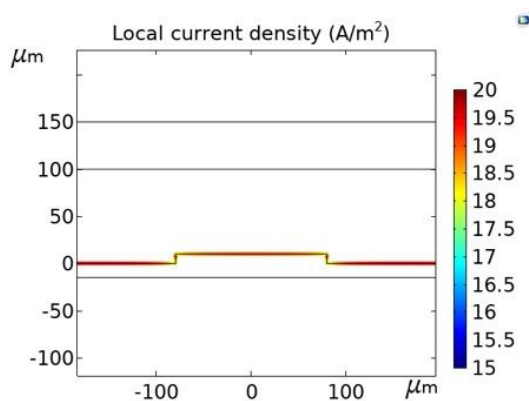


**Figure S11.** Cross-sectional views of local current densities over P-Cu using COMSOL simulation. Exchange current density value is corrected by the  $R_F$  values obtained from the Wenzel equation. The color bar indicates the local current density (unit: A m<sup>-2</sup>).

2). The local current density in the middle of the square-pattern and the receding region is  $\sim 19.0$  and  $\sim 19.3 \text{ A m}^{-2}$ , respectively.

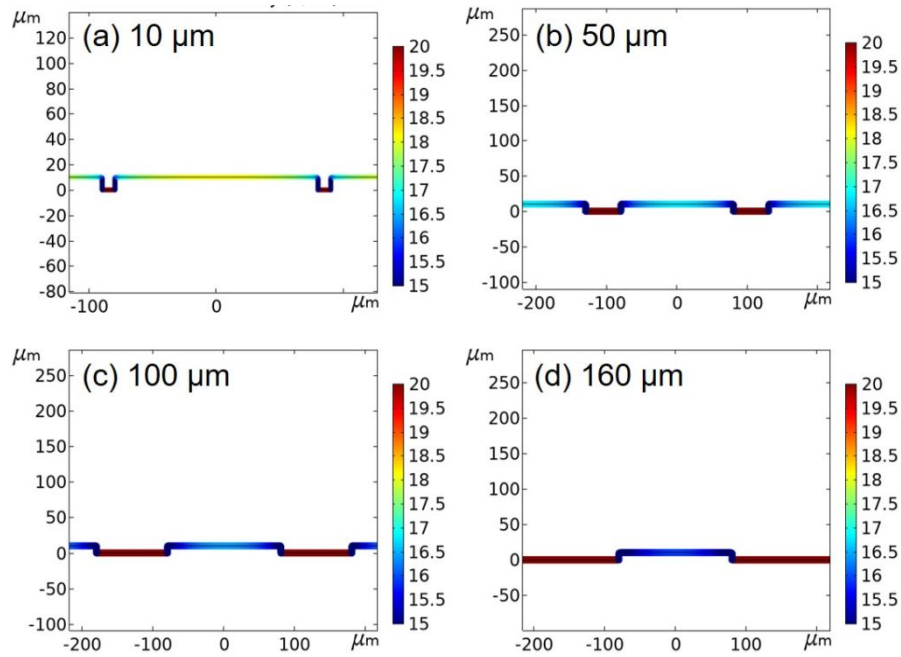


**Figure S12.** COMSOL simulation of local current density with different length of the receding parts, (a) 10, (b) 50, (c) 100, and (d) 160  $\mu\text{m}$ . The squared pattern sizes are 160  $\mu\text{m}$  and the depths are 15  $\mu\text{m}$  for all models. The surface roughness of 2 was set to the receding part.

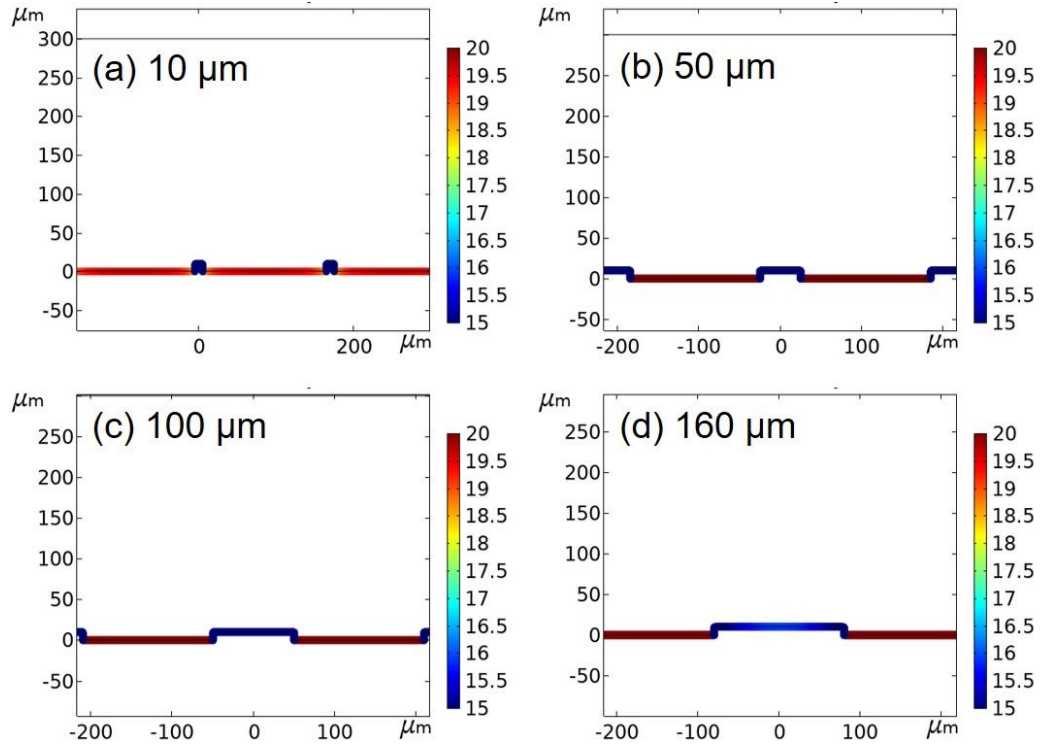


**Figure S13.** COMSOL simulation of local current density with different length of the squared pattern parts, (a) 10, (b) 50, (c) 100, and (d) 160  $\mu\text{m}$ . The lengths of the receding parts are 160  $\mu\text{m}$  and the depths are 15  $\mu\text{m}$  for all models. The surface roughness of 2 was set to the receding part.

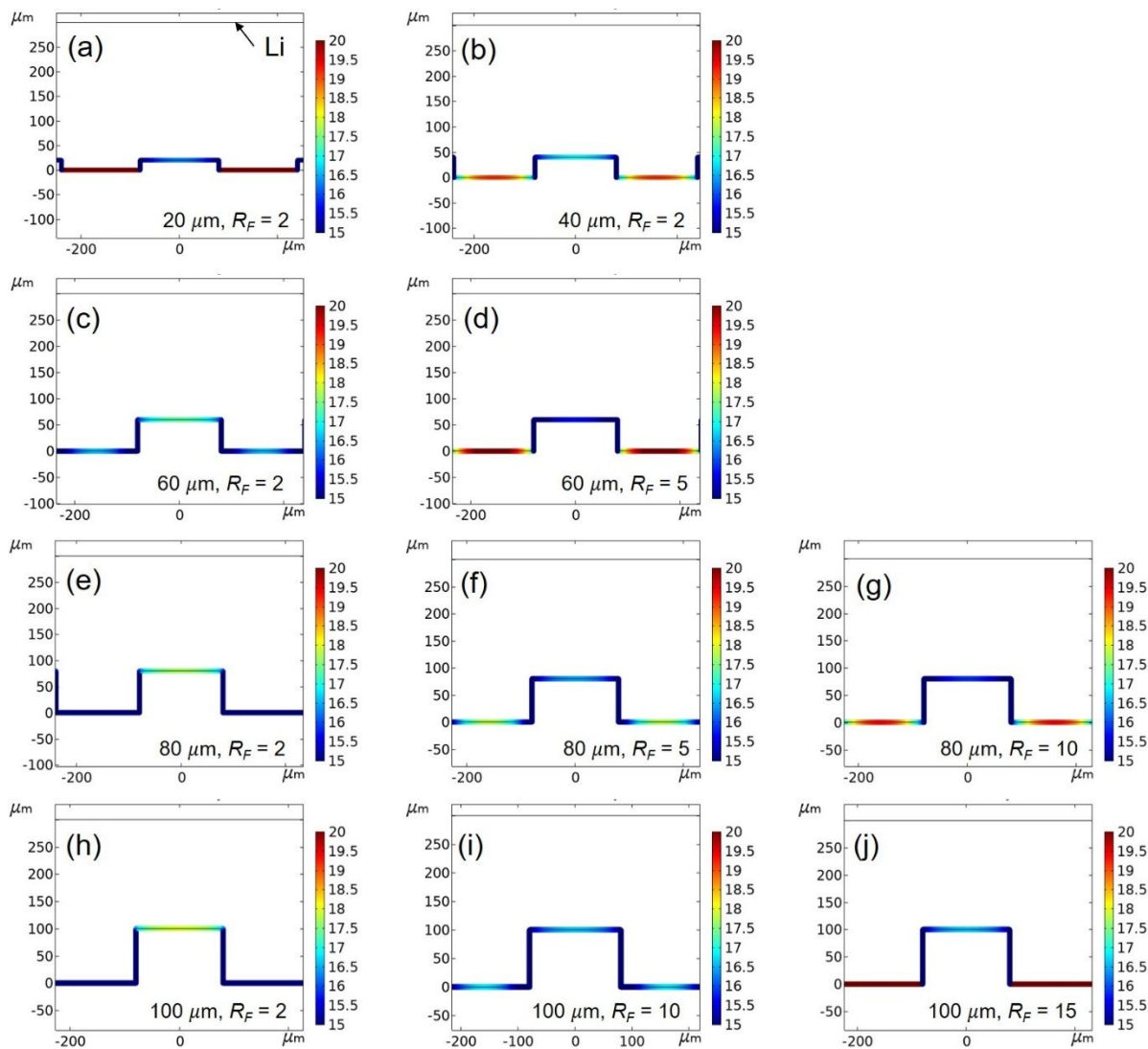


**Figure S14.** COMSOL simulation of local current density with different depth and roughness factor ( $R_F$ ), (a) 20  $\mu\text{m}$ ,  $R_F = 2$  (b) 40  $\mu\text{m}$ ,  $R_F = 2$  (c) 60  $\mu\text{m}$ ,  $R_F = 2$  (d) 60  $\mu\text{m}$ ,  $R_F = 5$  (e) 80  $\mu\text{m}$ ,  $R_F = 2$  (f) 80  $\mu\text{m}$ ,  $R_F = 5$  (g) 80  $\mu\text{m}$ ,  $R_F = 10$  (h) 100  $\mu\text{m}$ ,  $R_F = 2$  (i) 100  $\mu\text{m}$ ,  $R_F = 10$  (j) 100  $\mu\text{m}$ ,  $R_F = 15$ . The lengths of both the square-pattern and receding parts are 160  $\mu\text{m}$  for all models. In these simulations, the roughness factor was not included at the side edges of the square pattern.

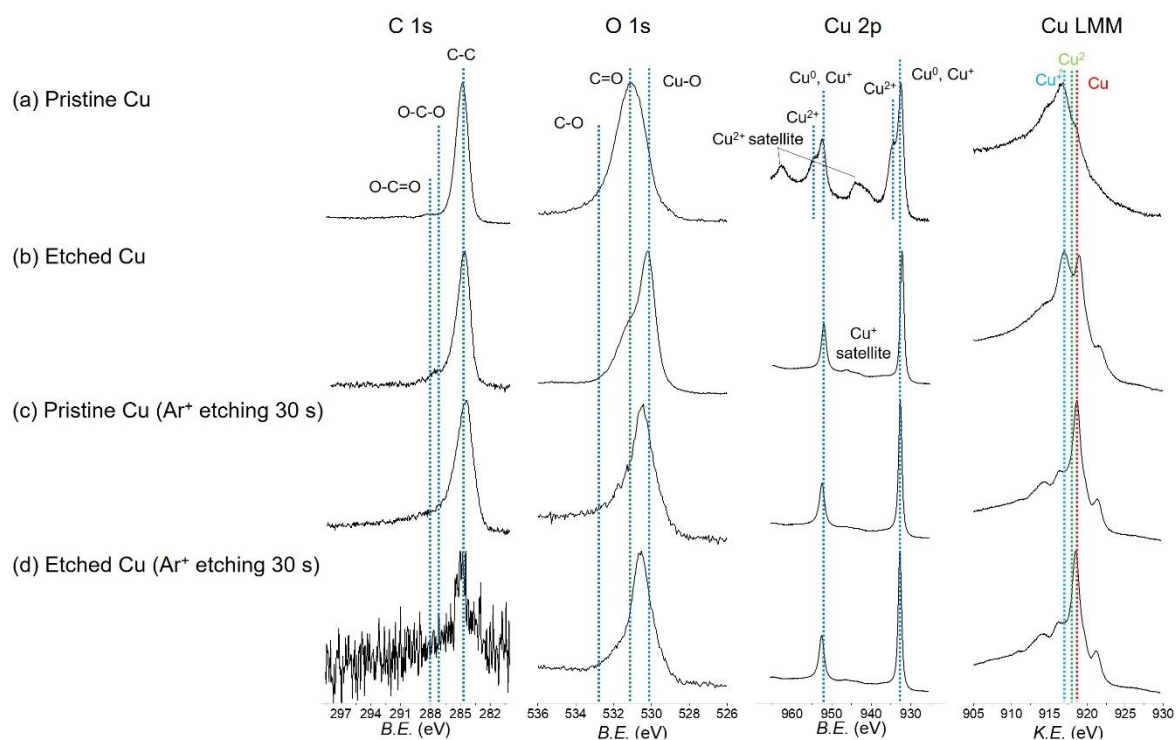


**Figure S15.** XPS spectra of C 1s, O 1s, Cu 2p binding energy (BE) regions, and Cu LMM spectra kinetic energy (KE) region for (a) pristine Cu, (b) etched Cu, (c) pristine Cu after 30 s Ar<sup>+</sup> etching, and (d) etched Cu after 30 s Ar<sup>+</sup> etching. The O-C=O, O-C-O, C-C (sp<sup>3</sup>) signals are assigned to 288.5, 286, and 284.8 eV, respectively, in the C 1s BE region.<sup>1</sup> In the O 1s BE region, C-O, C=O, and Cu-O signals appear at ~533, ~531, and ~530 eV, respectively.<sup>2</sup> The Cu<sup>2+</sup> signals emerge at 955 and 933.5 eV, and the Cu<sup>2+</sup> satellites are visible at 960 and 940 eV in the Cu 2p BE region. The Cu and Cu<sup>+</sup> signals are assigned to ~953 eV, and 933 eV. In the Cu LMM KE region, Cu<sup>+</sup>, Cu<sup>2+</sup>, Cu signals appear at 916.8, 917.7, and 918.6 eV, respectively.<sup>3</sup>



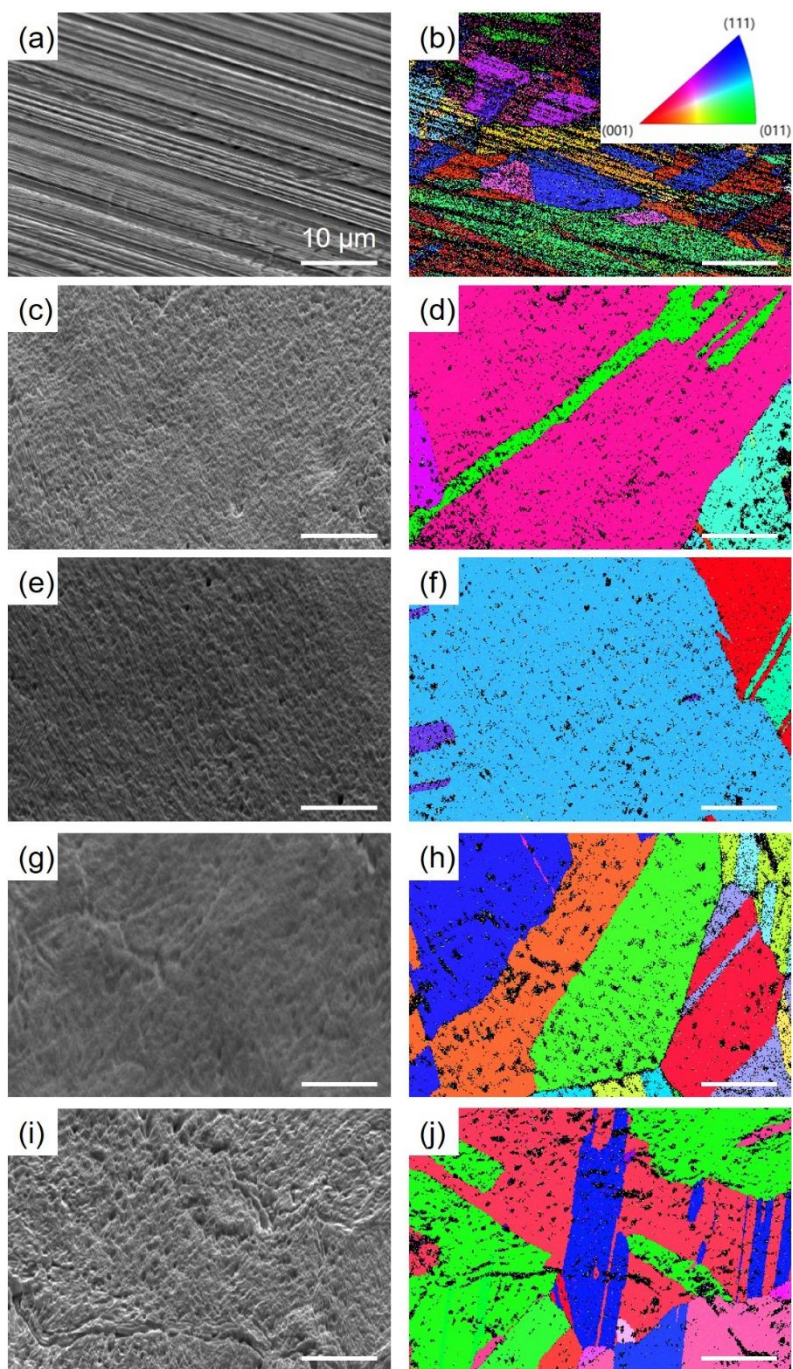


**Figure S16.** SEM images (left column) and corresponding electron backscatter diffraction (EBSD) in normal direction (IPFZ) images (right column). (a–b) Pristine Cu foil and (c–j) Etched Cu foil with various local areas. The insets in the EBSD are color



code for surface crystallinity of EBSD pattern. All scale bars indicate 10  $\mu\text{m}$ . Both pristine Cu and etched Cu have non-uniform surface crystal orientation.

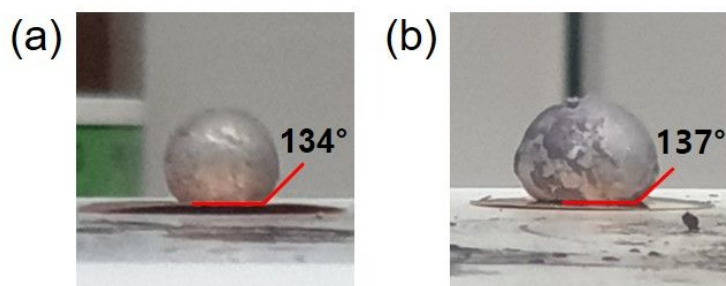


**Figure S17.** Contact angle measurements of molten Li on (a) etched Cu and (b) pristine Cu in an Ar-filled glovebox.

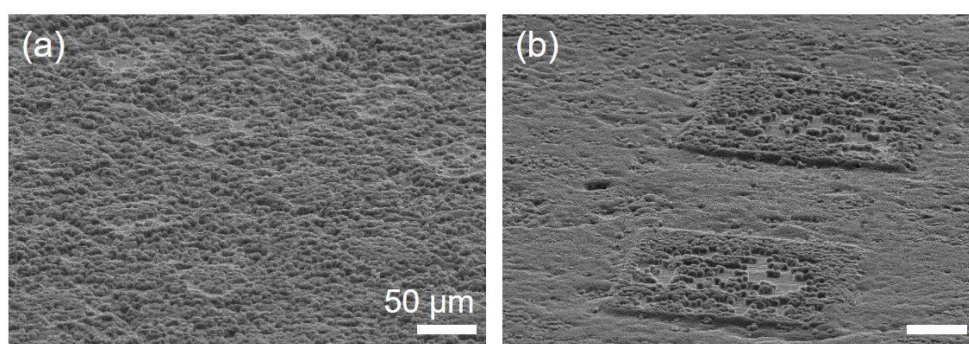


**Figure S18.** SEM images of P-Cu with (a) 80  $\times$  80  $\mu\text{m}^2$  and (b) 200  $\times$  200  $\mu\text{m}^2$  pattern after Li plating at a current density was 2  $\text{mA cm}^{-2}$  and a capacity was 1.0  $\text{mAh cm}^{-2}$ . All scale bars are 50  $\mu\text{m}$ .

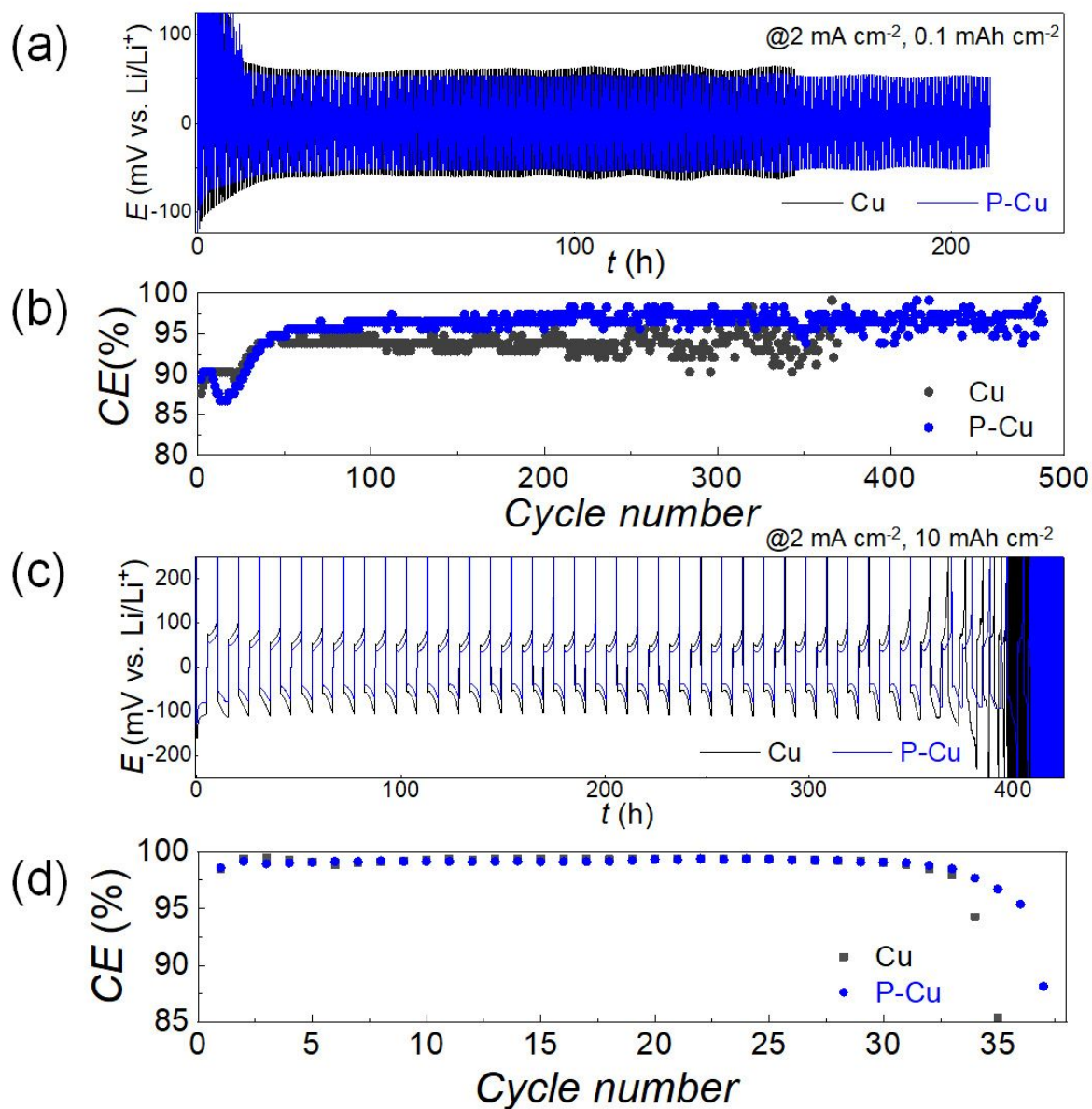


**Figure S19.** Comparative Li plating-stripping cyclability for pristine Cu (black) and P-Cu (blue) at a capacity of (a–b) 0.1 mAh cm<sup>-2</sup> and (c–d) 10 mAh cm<sup>-2</sup>. A current density was 2 mA cm<sup>-2</sup>, and the electrolyte solution was 1 M LiTFSI in DOL/DME with 1 wt% LiNO<sub>3</sub>. The effect of pattern is pronounced in the lower-capacity cycles. At 10 mAh cm<sup>-2</sup>, both Cu and P-Cu showed a similar cyclability. It is attributed to a shallow depth

of receding region ( $\sim 10 \mu\text{m}$ ) in the P-Cu we used, which was fully filled at  $1.0 \text{ mAh cm}^{-2}$  (Figure S18).

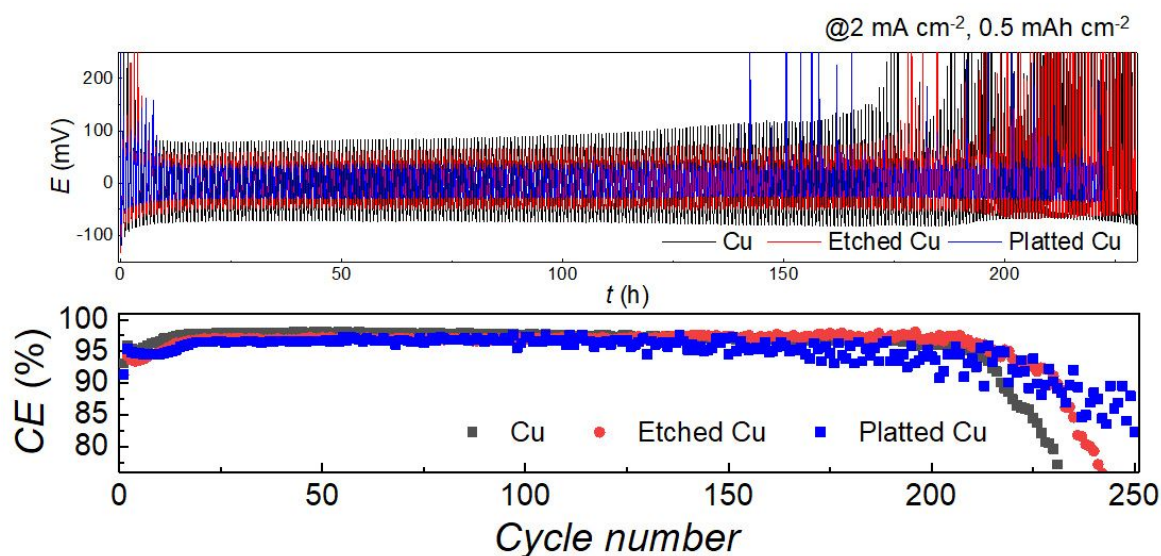


**Figure S20.** Comparative Li plating-stripping cyclability for pristine Cu (black), etched Cu (red), and platted Cu (blue) at a limited capacity of  $0.5 \text{ mAh cm}^{-2}$ . A current density was  $2 \text{ mA cm}^{-2}$  and the electrolyte solution was  $1 \text{ M LiTFSI}$  in DOL/DME with  $1 \text{ wt\% LiNO}_3$ .

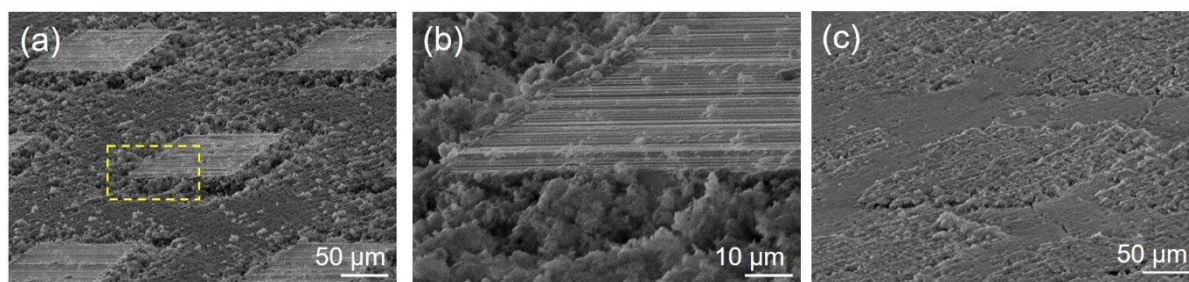


**Figure S21.** SEM images of the P-Cu with  $80 \times 80 \mu\text{m}^2$  pattern after (a–b) 10 cycles at a capacity of  $0.5 \text{ mAh cm}^{-2}$ , and (c) after 50 cycles at a capacity of  $0.5 \text{ mAh cm}^{-2}$ . A current density was  $2 \text{ mA cm}^{-2}$ . (b) is a high-magnification image of the dashed square box in (a).

## References

1. Ding, Y. F.; Zhang, F.; Xu, J. C.; Miao, Y. Q.; Yang, Y. Z.; Liu, X. G.; Xu, B. S., Synthesis of short-chain passivated carbon quantum dots as the light emitting layer towards electroluminescence. *RSC Adv.* 2017, 7(46), 28754-28762.
2. Oh, Y. J.; Yoo, J. J.; Kim, Y. I.; Yoon, J. K.; Yoon, H. N.; Kim, J. H.; Park, S. B., Oxygen functional groups and electrochemical capacitive behavior of incompletely reduced graphene oxides as a thin-film electrode of supercapacitor. *Electrochim. Acta* 2014, 116, 118-128.
3. Poulston, S.; Parlett, P. M.; Stone, P.; Bowker, M., Surface oxidation and reduction of CuO and Cu<sub>2</sub>O studied using XPS and XAES. *Surf. Interface Anal.* 1996, 24(12), 811-820.